


 Cite this: *RSC Adv.*, 2022, 12, 8668

Aldehyde *N,N*-dimethylhydrazone-based fluorescent substrate for peroxidase-mediated assays†

Soyeon Yoo, Sudeok Kim, Sangyeon Jeon and Min Su Han *

Numerous assays based on peroxidase activity have been developed for the detection of analytes due to the various optical peroxidase substrates. However, most substrates are sensitive to light and pH and are over-oxidized in the presence of excess H₂O₂. In this study, 2-((6-methoxynaphthalen-2-yl)methylene)-1,1-dimethylhydrazine (MNDH), a fluorescent peroxidase substrate prepared from naphthalene-based aldehyde *N,N*-dimethylhydrazone, was developed. MNDH showed quantitative fluorescence changes with respect to the H₂O₂ concentration in the presence of horseradish peroxidase (HRP), and the MNDH/HRP assay showed no changes in fluorescence caused by over-oxidation in the presence of excess H₂O₂. Further, MNDH was thermo- and photostable. Additionally, the assay could be operated over a considerably wide pH range, from acidic to neutral. Moreover, MNDH can be used to detect glucose quantitatively in human serum samples by using an enzyme cascade assay system.

 Received 6th January 2022
 Accepted 22nd February 2022

DOI: 10.1039/d2ra00087c

rsc.li/rsc-advances

Introduction

Peroxidase activity, which involves the oxidation of organic substrates with the aid of H₂O₂, is extensively utilized in various bio-sensors, such as multi-enzyme cascade-based assays and enzyme-linked immunosorbent assays.^{1–3} The widespread application of peroxidases in sensing systems can be attributed to (1) the large number of optical peroxidase substrates, (2) the very high turnover numbers of these catalyst systems, and (3) the ease of combining peroxidases with other enzymes that produce H₂O₂ as a byproduct.⁴ Horseradish peroxidase (HRP), a natural heme-containing enzyme, is one of the most commonly used enzymes in sensing systems owing to its high specificity, sensitivity, and stability for conjugation with antibodies.^{4–6} HRP is oxidized to oxHRP by using hydrogen peroxide, which then catalyzes the oxidation of the optical substrate, while oxHRP is reduced to HRP.⁷ The resulting changes in the optical properties of the substrate enable qualitative and quantitative analyses of the analyte.

As optical substrates undergo changes in color, fluorescence, or chemiluminescence in the presence of peroxidases, these systems have been widely applied in sensing systems. Commonly used peroxidase substrates include colorimetric substrates such as 2,2'-azino-bis(3-ethylbenzothiazoline-6-sulfonate) (ABTS) and 3,3',5,5'-tetramethylbenzidine (TMB), fluorescent substrates such as Amplex Red, and

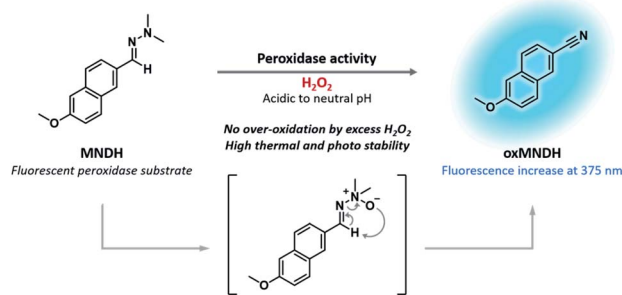
chemiluminescent substrates such as luminol.^{8–11} Thus, a wide range of substrates having different optical properties exists, and suitable substrates can be selected in accordance with assay operating conditions such as pH. Colorimetric substrates are mainly used in acidic-to-neutral conditions, and the color changes are detectable by the naked eye.^{12–14} However, in complex matrices such as biological samples, the colored radical products of ABTS and TMB formed through peroxidase-mediated oxidation can react with other antioxidants, resulting in a loss of color.^{15,16} In contrast, fluorescent and chemiluminescent substrates have higher sensitivities, and thus, lower concentrations can be used.^{17–19} However, fluorescent substrates such as Amplex Red can only be used at pH 7–8 because oxidized Amplex Red, a fluorescent resorufin, is further oxidized to the non-fluorescent resazurin under acidic conditions.²⁰ The chemiluminescence of luminol is also inhibited at an acidic pH.²¹ In addition, in the case of Amplex Red, if a small amount of its product (resorufin) is present, photo-oxidation occurs even in the absence of H₂O₂, thereby lowering the detection sensitivity.²² Moreover, these common substrates are excessively oxidized by high concentrations of H₂O₂, resulting in a loss of color or fluorescence.^{23,24} Hence, new fluorescent peroxidase substrates must be (1) universally applicable at an acidic-to-neutral pH, (2) photostable, and (3) not overly oxidized by excess H₂O₂.

In this study, 2-((6-methoxynaphthalen-2-yl)methylene)-1,1-dimethylhydrazine (MNDH) was developed as a new fluorescent peroxidase substrate that can be used under acidic-to-neutral pH conditions. MNDH was designed by combining the reactive aldehyde *N,N*-dimethylhydrazone moiety and the fluorophore methoxynaphthalene (Scheme 1). *N,N*-

Department of Chemistry, Gwangju Institute of Science and Technology (GIST), Gwangju 61005, Republic of Korea. E-mail: happyhan@gist.ac.kr

† Electronic supplementary information (ESI) available. See DOI: 10.1039/d2ra00087c





Scheme 1 Structure of MNDH, a new fluorescent peroxidase substrate, and the proposed mechanism of the peroxidase-catalyzed oxidation of MNDH in the presence of H_2O_2 .

Dimethylhydrazone is a well-known protecting group for ketones but is not used to protect aldehydes because complete deprotection is difficult.²⁵ The aldehyde *N,N*-dimethylhydrazone moiety can be oxidized by employing H_2O_2 in the presence of methyltrioxorhenium (MTO) as a catalyst to form an *N*-oxide intermediate, which is converted to a nitrile through the Cope elimination reaction.^{26,27} This reaction was performed under mild conditions using a small amount of acetic acid. Because HRP mainly oxidizes the amine group of common substrates with the help of H_2O_2 , we speculated that, instead of MTO, HRP could be used to catalyze the oxidation of *N,N*-dimethylhydrazone under mild conditions at an acidic pH. In that case, the nitrile group formed by the oxidation reaction would not be overly oxidized by the remaining H_2O_2 , thus solving the over-oxidation problem.²⁶ As expected, MNDH was oxidized by HRP and H_2O_2 to form oxMNDH with a nitrile group, resulting in an increase in the fluorescence intensity at 375 nm. Based on this change in fluorescence, we found that MNDH can be used to measure the peroxidase activity of HRP at pH 4 and 7, and we confirmed that there was no change in the nonspecific fluorescence signal arising from the presence of excessive H_2O_2 or light and heat.

Experimental

Materials and instrumentation

Chemical reagents were purchased from commercial sources (Sigma-Aldrich, Tokyo Chemical Industry, and Duksan Pure Chemical, Korea) and used without further purification. Human serum was purchased from Sigma-Aldrich. ^1H and ^{13}C nuclear magnetic resonance (NMR) spectra were recorded using a JEOL 400 MHz NMR spectrometer. High-resolution mass spectra (HRMS) were recorded using a Bruker Impact II quadrupole time-of-flight (QToF) mass spectrometer with an electrospray ionization (ESI) source. Melting point analysis was performed using a Büchi M-560 melting point apparatus. The fluorescence spectra were recorded using an Agilent Cary Eclipse fluorescence spectrophotometer, and absorbance spectra were recorded on a JASCO V-630 UV-Vis spectrophotometer. Fourier-transform infrared (FTIR) spectra were recorded on a Thermo Scientific NICOLET iS10 spectrometer using a KBr disc (Thermo Scientific, 25×4 mm).

Synthesis of 2-((6-methoxynaphthalen-2-yl)methylene)-1,1-dimethylhydrazine (MNDH)

6-Methoxy-2-naphthaldehyde (10 mmol, 1.86 g) was dissolved in 30 mL of dichloromethane containing anhydrous magnesium sulfate (20 mmol, 2.41 g), *N,N*-dimethylhydrazine hydrochloride (20 mmol, 1.45 g), and trimethylamine (7 mmol, 0.98 mL). The mixture was then stirred for 10 h at room temperature. Subsequently, the mixture was washed three times with a saturated NaHCO_3 (aq.) solution and brine. Then, the organic layer was dried using sodium sulfate and concentrated under reduced pressure. The mixture was then purified by applying flash column chromatography (CHCl_3 : MeOH = 100 : 1), followed by two-solvent recrystallization (ethyl acetate/hexane) to yield a white crystalline solid (1.62 g, yield 70.96%). $^1\text{H-NMR}$ (400 MHz, $\text{DMSO-}D_6$) δ 7.81–7.72 (m, 4H), 7.43 (s, 1H), 7.28 (d, $J = 2.5$ Hz, 1H), 7.13 (dd, $J = 8.9, 2.5$ Hz, 1H), 3.86 (s, 3H), 2.93 (s, 6H). $^1\text{H-NMR}$ (400 MHz, acetonitrile ($\text{ACN-}D_3$)) δ 7.82 (dd, $J = 8.5, 1.5$ Hz, 1H), 7.77 (s, 1H), 7.73 (dd, $J = 12.4, 8.7$ Hz, 2H), 7.43 (s, 1H), 7.24 (d, $J = 2.4$ Hz, 1H), 7.13 (dd, $J = 9.0, 2.6$ Hz, 1H), 3.92–3.87 (3H), 2.97–2.93 (6H). $^{13}\text{C-NMR}$ (101 MHz, $\text{DMSO-}D_6$) δ 157.2, 133.7, 132.5, 132.4, 129.2, 128.5, 126.9, 124.8, 123.3, 118.7, 106.2, 55.2, 42.6. HRMS (ESI): $[\text{M} + \text{H}]^+ m/z$ calculated for $\text{C}_{14}\text{H}_{17}\text{N}_2\text{O}$: 229.1335; found: 229.1333. Melting point: 144.1–144.8 °C.

pH screening of the MNDH/HRP system

MNDH (20 μM , ACN 5%) was added to various buffer solutions (20 mM) having different pH ranges (4.0–5.0 (acetate), 6.0 (MES), and 7.0–9.0 (Tris-HCl)), containing HRP (50 mU mL^{-1}) and H_2O_2 (0 or 50 μM). Fluorescence spectra were recorded over 1 h at 2 min intervals at 25 °C.

Study of the operating mechanism of the MNDH/HRP system

Combinations of MNDH (20 μM , ACN 5%), HRP (50 mU mL^{-1}), and H_2O_2 (50 μM) were added to an acetate buffer solution (20 mM) of pH 4.0, and the fluorescence spectra of samples were recorded at 25 °C for 5 min.

For large-scale sample preparation, MNDH (100 μM , ACN 5%), HRP (250 mU mL^{-1}), and H_2O_2 (250 μM) in a pH 4.0 buffer solution (acetate, 20 mM) were placed in a 500 mL volumetric flask. The mixture was extracted three times by using chloroform. The organic layer was then collected and concentrated under reduced pressure, and the oxMNDH was obtained by performing column chromatography using chloroform. $^1\text{H-NMR}$ (400 MHz, $\text{ACN-}D_3$) δ 8.27 (s, 1H), 7.89 (t, $J = 8.9$ Hz, 2H), 7.62 (dd, $J = 8.5, 1.8$ Hz, 1H), 7.35 (d, $J = 2.4$ Hz, 1H), 7.28 (dd, $J = 8.9, 2.4$ Hz, 1H), 3.94 (s, 3H). $^{13}\text{C-NMR}$ (101 MHz, $\text{ACN-}D_3$) δ 161.1, 137.5, 134.8, 131.0, 128.9, 128.6, 128.0, 121.5, 120.4, 107.4, 107.1, 56.3. The FTIR spectra of MNDH and oxMNDH were obtained by using the KBr disc method.

MNDH and H_2O_2 titration using the MNDH/HRP system

MNDH (0 to 30 μM , ACN 5%) was added to a buffer solution (acetate pH 4.0 or Tris-HCl pH 7.0, 20 mM) containing HRP (50 mU mL^{-1}) and H_2O_2 (50 μM), and the fluorescence spectra



were recorded at 25 °C at 15 s intervals over 10 min for the pH 4.0 and 60 min for the pH 7.0.

H₂O₂ (0–30 or 20 μM) was added to buffer solution (acetate pH 4.0 or Tris–HCl pH 7.0, 20 mM) containing HRP (50 mU mL⁻¹) and **MNDH** (20 μM, ACN 5%), and fluorescence spectra were recorded at 25 °C at 15 s intervals over 10 min for the pH 4.0 and 60 min for the pH 7.0.

The initial reaction velocity (V_0) was calculated from the initial linear change in the fluorescence intensity from 0 to 60 s at pH 4.0 and from 0 to 5 min at pH 7.0. The Michaelis–Menten constant (K_m) and maximum reaction velocity (V_{max}) were obtained from the Lineweaver–Burk plot.

Thermo- and photostability of **MNDH**

A batch of **MNDH** solutions (400 μM, ACN 100%) was incubated for 6 h at 60 °C on a hot plate. Another batch of **MNDH** solutions (400 μM, ACN 100%) was incubated for 24 h in a light-box with a 25 W light-emitting diode lamp (6000 K). Then, the **MNDH** (20 μM, ACN 5%) incubated on the hot plate or in a light-box was added to the buffer solution (acetate pH 4.0 or Tris–HCl pH 7.0, 20 mM) containing HRP (50 mU mL⁻¹) and H₂O₂ (50 μM), and fluorescence spectra were recorded at 25 °C for 5 min for the pH 4.0 and 30 min for the pH 7.0.

Application of the **MNDH**/HRP system for glucose detection

Glucose (0–100 μM) was added to a buffer solution (Tris–HCl pH 7.0, 20 mM) containing HRP (0.1 U mL⁻¹), glucose oxidase (GOx) (0.5 U mL⁻¹), and **MNDH** (20 μM, ACN 5%), and fluorescence spectra were recorded at 25 °C for 60 min at 30 s intervals.

Selectivity for glucose over other saccharides

Various saccharides (50 μM glucose and 500 μM each of galactose (Gal), fructose (Fru), maltose (Mal), lactose (Lac), and sucrose (Suc)) were added to a buffer solution (Tris–HCl pH 7.0, 20 mM) containing HRP (0.1 U mL⁻¹), GOx (0.5 U mL⁻¹), and **MNDH** (20 μM, ACN 5%), and fluorescence spectra were recorded at 25 °C for 60 min at 30 s intervals.

Serum glucose assay using the **MNDH**/HRP system

Human serum samples were prepared by applying ultrafiltration and diluted by a factor of 37.5. The samples were then added to the buffer solution (Tris–HCl pH 7.0, 20 mM) containing HRP (0.1 U mL⁻¹), GOx (0.5 U mL⁻¹), and **MNDH** (20 μM, ACN 5%), and fluorescence spectra were recorded at 25 °C for 30 min at 30 s intervals.

Results and discussion

Synthesis and characterization of **MNDH** as the peroxidase substrate

MNDH was synthesized in a single step, yielding a white crystalline solid, and the ¹H- and ¹³C-NMR spectra, HRMS, and melting point data (Fig. S1–S3†) confirmed that **MNDH** had been cleanly synthesized. After synthesis, we investigated the pH range over which **MNDH** can be used as a peroxidase

substrate *via* reaction with H₂O₂. Under various pH conditions (pH 4.0 to 9.0), time-dependent changes in the fluorescence of **MNDH** solutions containing HRP were observed in both the presence and absence of H₂O₂ (Fig. S4†). In the absence of H₂O₂, no change was observed in the fluorescence of the solution over time, regardless of the pH. In the presence of H₂O₂, the use of a lower pH resulted in a rapid increase in the fluorescence intensity of the solution over time. In particular, the fluorescence signal was saturated within 3 min at pH 4.0. Although the change in the absolute fluorescence intensity of the solution at pH 7.0 was slower and lower than that at pH 4.0, the difference in the fluorescence intensity in the presence of H₂O₂ was approximately 65-times greater after 5 min than that in its absence (at pH 7.0). This is because the fluorescence intensity at 375 nm for **MNDH** was almost zero at pH 7.0. Consequently, **MNDH** can be used as a fluorescent substrate in acidic-to-neutral solutions.

Mechanistic study of **MNDH**

To determine the mechanism of the **MNDH**/HRP system, the changes in the fluorescence of **MNDH** in a pH 4.0 buffer solution containing a combination of HRP and H₂O₂ were observed. The fluorescence spectra of the **MNDH** solutions containing either HRP or H₂O₂ were consistent with those of the **MNDH** solutions without both HRP and H₂O₂ (Fig. 1). In contrast, for the **MNDH** solution containing both HRP and H₂O₂, the fluorescence intensity at 375 nm increased significantly. Thus, the fluorescence of **MNDH** was affected only in the presence of both HRP and H₂O₂. This indicates that oxHRP, which is formed in the presence of H₂O₂, catalyzes the oxidation of **MNDH**, suggesting that **MNDH** can be used as a new fluorescent substrate for peroxidases. To confirm the structure of the oxidized form of **MNDH** (ox**MNDH**) formed in the presence of H₂O₂ and HRP, a large-scale sample was prepared, and ¹H- and ¹³C-NMR and FTIR measurements were performed. As shown in the ¹H-NMR spectra (Fig. S2 and S5†), the peaks corresponding to the dimethyl and N=CH moieties of the dimethylhydrazone group of **MNDH** disappear after oxidation to yield ox**MNDH**. In

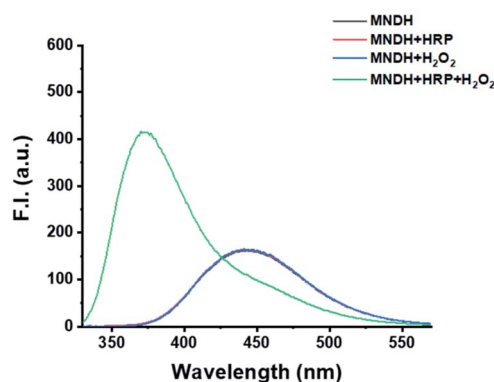


Fig. 1 Fluorescence spectra of **MNDH** in buffer solution containing various combinations of HRP and H₂O₂. [**MNDH**] = 20 μM, [H₂O₂] = 50 μM, [HRP] = 50 mU mL⁻¹, [acetate pH 4.0] = 20 mM. F.I. = fluorescence intensity.



addition, in the ^{13}C -NMR spectra (Fig. S6†), no peaks corresponding to the dimethyl group are observed. Furthermore, the obtained NMR spectra of oxMNDH are found to be consistent with the NMR spectra of 6-methoxy-2-naphthonitrile (Fig. S7 and S8†),^{27,28} and the IR spectrum of oxMNDH contains a new peak at 2222 cm^{-1} , which can be attributed to a $\text{C}\equiv\text{N}$ group (Fig. S9†). These results reveal that oxMNDH has the structure of 6-methoxy-2-naphthonitrile ($\text{C}_{12}\text{H}_9\text{NO}$). Therefore, we conclude that the *N,N*-dimethylhydrazone moiety in MNDH was oxidized to a nitrile group in the presence of HRP and H_2O_2 *via* the Cope elimination reaction per our original design.

Kinetic study of the enzymatic reaction and H_2O_2 detection in the MNDH/HRP system

Next, a kinetic study of the peroxidase reaction was conducted using MNDH as the peroxidase substrate. The samples were prepared by fixing the concentration of either MNDH or H_2O_2 while changing the concentration of the other; these experiments were performed in a pH 4.0 or 7.0 buffer solution containing HRP. Concentration-dependent fluorescence of the assay was observed for both MNDH and H_2O_2 . In particular, as the concentration of MNDH or H_2O_2 increased, the fluorescence intensity of the solution and the initial rate (V_0) of the enzymatic reaction increased (Fig. 2, S10 and S11†). At pH 4.0, MNDH was rapidly oxidized by HRP and H_2O_2 to the extent that the fluorescence intensity was saturated within approximately 3 min, and the fluorescence increased significantly when the MNDH

concentration was 20–30 μM (Fig. 2a and S10†). In addition, for H_2O_2 concentrations of 0–15 μM , the concentration-dependent change in the fluorescence intensity was linear, and the limit of detection (LOD) reached as low as 0.03 μM (Fig. 2b and S12a†). At pH 7.0, the fluorescence intensity increased relatively slowly with time (Fig. S11†). The increase was linear between H_2O_2 concentrations of 0 and 7.5 μM , and the LOD was 0.06 μM (Fig. 2b and S12b†). As shown by these LOD values, low concentrations of H_2O_2 can be detected by the MNDH/HRP system. Next, we used the Michaelis–Menten equation to obtain the kinetic parameters. When the reciprocal of V_0 was plotted against the reciprocal of MNDH or H_2O_2 concentration, linear plots having excellent correlation coefficients (R^2 ; 0.956–0.996) were obtained. As shown in Table 1, K_m and V_{max} are 18.14 μM and $0.38\ \Delta\text{F s}^{-1}$, respectively, for H_2O_2 , and 0.66 μM and $7.11\ \Delta\text{F s}^{-1}$, respectively, for MNDH, at pH 4.0. These K_m values are much lower than those of other widely used colorimetric substrates (for example,

Table 1 Comparison of the kinetic parameters of HRP depending on MNDH and H_2O_2 concentrations, including Michaelis–Menten constants (K_m) and maximum reaction rates (V_{max}) at pH 4.0 and 7.0

Enzyme	pH	Substrate	K_m (μM)	V_{max} ($\Delta\text{F s}^{-1}$)
HRP	4.0	H_2O_2	18.14	0.38
		MNDH	0.66	7.11
	7.0	H_2O_2	313.19	0.08
		MNDH	952.70	0.20

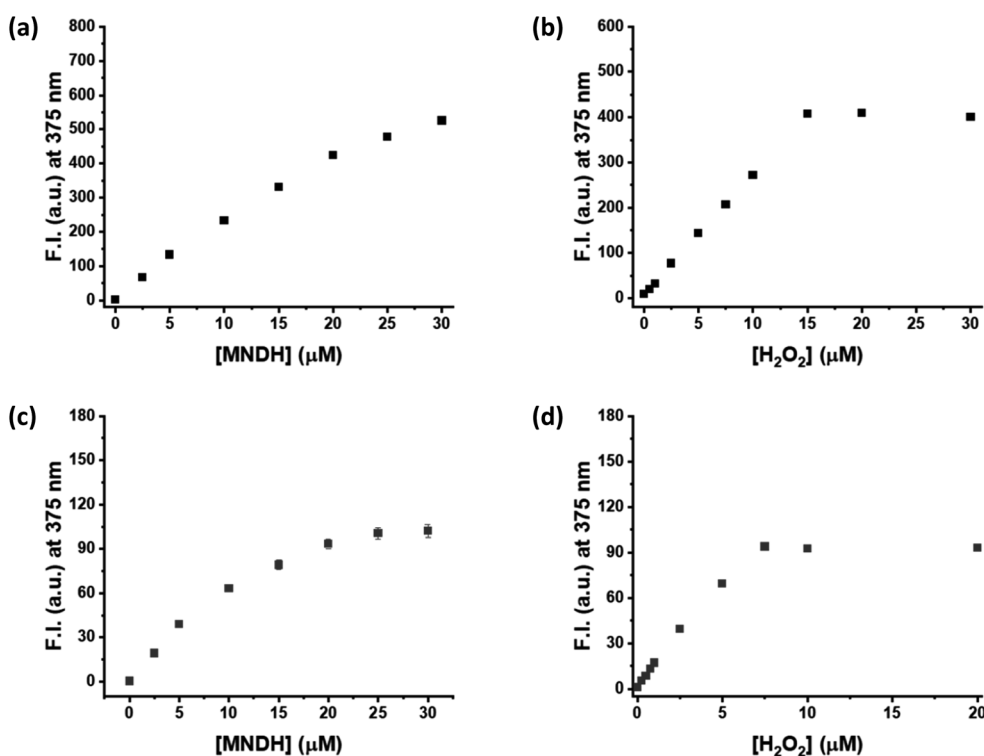


Fig. 2 Fluorescence intensity (F.I.) versus concentration for assays of (a and c) MNDH or (b and d) H_2O_2 at a fixed concentration of the other in the presence of HRP at (a and b) pH 4.0 or (c and d) pH 7.0. $[\text{MNDH}] = 20\ \mu\text{M}$, $[\text{H}_2\text{O}_2] = 50\ \mu\text{M}$, $[\text{HRP}] = 50\ \text{mU mL}^{-1}$, [acetate pH 4.0, Tris–HCl pH 7.0] = 20 mM.



0.434 mM for TMB and 3.70 mM for H₂O₂) but similar to those for Amplex Red.^{29,30} Unfortunately, the K_m value for **MNDH** is rather high at pH 7.0, although that for H₂O₂ is low: 313.19 μ M. Moreover, in the presence of excess H₂O₂, the saturated fluorescence signal of ox**MNDH** remains high for a long period, suggesting that ox**MNDH** is not over-oxidized by the remaining H₂O₂ (Fig. S10a and b†). Hence, these results indicate that **MNDH** is a promising new fluorescent peroxidase substrate.

Thermo- and photostability of **MNDH**

The stability of the peroxidase substrate in the presence of light and heat during storage and use is crucial because, on receiving energy from these sources, unstable substrates can undergo a range of reactions that can diminish their fluorescence properties. These problems reduce the accuracy and precision of analyte detection, thereby affecting the reliability of the assay. For example, Amplex Red, which is a widely used substrate, has low photostability and requires protection from light during use, making it an inconvenient reagent. To verify the thermostability of our system, the **MNDH** solution was heated on a hot plate at 60 °C for 6 h and then cooled to room temperature. The change in the fluorescence of the **MNDH** solution after adding it to a combination of H₂O₂ and HRP in a pH 4.0 buffer solution was then measured at 25 °C (Fig. 3). The fluorescence signal of the sample containing preheated **MNDH** was similar to that of unheated **MNDH**, indicating thermostability. Next, the photostability of **MNDH** was tested. After exposure to 25 W, 6000 K light for 24 h in a light-box, the fluorescence of the **MNDH** solution was measured using the same method as that used for the thermostability experiments; no changes were observed, indicating that the **MNDH** solution is photostable. Further, in the absence of HRP and H₂O₂, the light-irradiated **MNDH** showed no changes in fluorescence, indicating that the **MNDH** had not been photo-oxidized. These results were also observed at pH 7.0 (Fig. S13†). Although **MNDH** had a lower emission wavelength than previously reported fluorescent peroxidase substrates such as Amplex Red, it exhibited comparatively higher thermo- and photostability.^{31–34} Therefore, as a result of its easier storage, **MNDH** can be used as a substitute for Amplex Red.

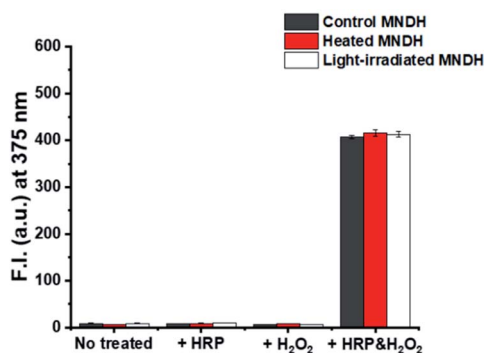


Fig. 3 Fluorescence intensity (F.I.) of **MNDH** previously exposed to heat and light in buffer solutions containing various combinations of HRP and H₂O₂. [**MNDH**] = 20 μ M, [H₂O₂] = 50 μ M, [HRP] = 50 mU mL⁻¹, [acetate pH 4.0] = 20 mM.

Application of **MNDH** for glucose detection

Finally, a model study based on glucose detection was conducted to confirm if **MNDH** can be applied as a peroxidase substrate for multi-enzyme cascade assays. After glucose was added at various concentrations to a pH 7.0 buffer solution containing GOx, HRP, and **MNDH**, the fluorescence intensity was measured. As the glucose concentration increased, the fluorescence intensity increased and, finally, became saturated (Fig. 4a and S14a†). The plot of fluorescence intensity *versus* glucose concentration showed excellent linearity ($R^2 = 0.987$) between glucose concentrations of 0 and 20 μ M, having a low LOD of 0.31 μ M (Fig. S15†). In addition, the selectivity of the **MNDH**/GOx/HRP assay for glucose in the presence of other saccharides, including Gal, Fru, Mal, Lac, and Suc, was tested. The concentrations of the other saccharides were maintained at 10 times the concentration of glucose. After the samples were prepared in the same manner as the glucose titration, the fluorescence intensities of the samples were measured. As shown in Fig. 4b and S14b,† unlike glucose, the other saccharides do not cause any significant increase in fluorescence, indicating that the **MNDH**/GOx/HRP assay system is highly glucose-specific. The applicability of the **MNDH**/GOx/HRP assay system to human serum samples was also tested. Human serum samples were purchased from Sigma-Aldrich and prepared by applying ultrafiltration to remove proteins. The **MNDH**/GOx/HRP assay system was used to determine the concentration of

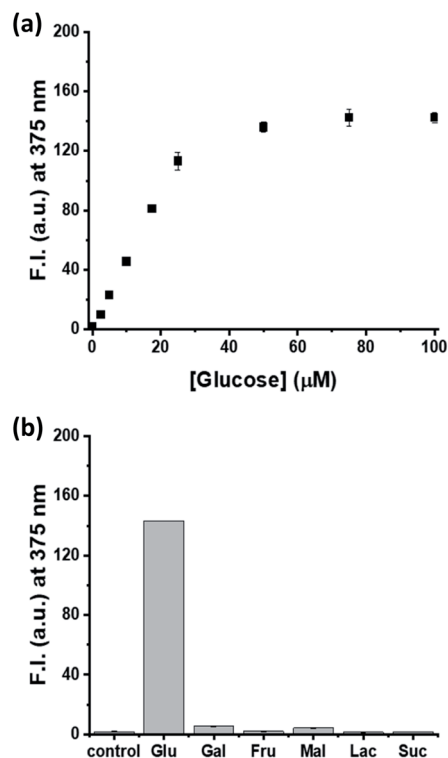


Fig. 4 Fluorescence intensity (F.I.) of assay solutions *versus* (a) concentration of glucose or (b) type of saccharide. [**MNDH**] = 20 μ M, [glucose] = 50 μ M, [other saccharide] = 500 μ M, [HRP] = 100 mU mL⁻¹, [GOx] = 500 mU mL⁻¹, [Tris-HCl pH 7.0] = 20 mM.



glucose in human serum to be 5.04 ± 0.01 mM, which was nearly identical to that (5.19 ± 0.03 mM) measured by using a glucose meter. Thus, the proposed system can accurately measure the concentration of glucose in human serum, indicating its potential for application in the diagnosis of diseases for which glucose is a biomarker.

Conclusions

MNDH, a new fluorescent peroxidase substrate based on the aldehyde *N,N*-dimethylhydrazone, was developed. The synthesis of **MNDH** is simple in a single step and requires commercially available reagents. **MNDH** was oxidized to fluorescent ox**MNDH** containing a cyano group by using HRP and H₂O₂, and the **MNDH**/HRP assay system can be operated at an acidic-to-neutral pH. Further, the detection of H₂O₂ at micromolar levels is possible. **MNDH** showed considerable thermo- and photostability and was not over-oxidized in the presence of excess H₂O₂. Moreover, **MNDH** can be applied to an enzyme cascade assay system for the detection of glucose in human serum. Thus, **MNDH** is expected to replace existing peroxidase substrates in various sensing fields.

Author contributions

Soyeon Yoo: data curation, formal analysis, investigation, methodology, validation, visualization, writing – original draft, writing – review & editing. Sudeok Kim: data curation, investigation. Sangyeon Jeon: methodology, resources. Min Su Han: conceptualization, funding acquisition, project administration, supervision, writing – review & editing.

Conflicts of interest

There are no conflicts to declare.

Acknowledgements

This research was supported by the National Research Foundation of Korea (NRF) grant funded by the Korea government (MSIT) (NRF-2020R1A2B5B01002392).

Notes and references

- V. P. Pandey, M. Awasthi, S. Singh, S. Tiwari and U. N. Dwivedi, *Biochem. Anal. Biochem.*, 2017, **6**, 1000308.
- H. Zhang and S. Wang, *J. Immunol. Methods*, 2009, **350**, 1–13.
- G. Palazzo, G. Colafemmina, C. Guzzoni Iudice and A. Mallardi, *Sens. Actuators, B*, 2014, **202**, 217–223.
- A. M. Azevedo, V. C. Martins, D. M. F. Prazeres, V. Vojinović, J. M. S. Cabral and L. P. Fonseca, *Biotechnol. Annu. Rev.*, 2003, **9**, 199–247.
- H. Nakajima, M. Yagi, Y. Kudo, T. Nakagama, T. Shimosaka and K. Uchiyama, *Talanta*, 2006, **70**, 122–127.
- K. Y. Xing, J. Peng, S. Shan, D. F. Liu, Y. N. Huang and W. H. Lai, *Anal. Chem.*, 2020, **92**, 8422–8426.
- N. C. Veitch, *Phytochemistry*, 2004, **65**, 249–259.
- P. D. Josephy, T. Eling and R. P. Mason, *J. Biol. Chem.*, 1982, **257**, 3669–3675.
- R. E. Childs and W. G. Bardsley, *Biochem. J.*, 1975, **145**, 93–103.
- K. J. Reszka, B. A. Wagner, C. P. Burns and B. E. Britigan, *Anal. Biochem.*, 2005, **342**, 327–337.
- G. Thorpe, L. J. Kricka, S. Moseley and T. P. Whitehead, *Clin. Chem.*, 1985, **31**, 1335–1341.
- H.-F. Lu, J.-Y. Li, M.-M. Zhang, D. Wu and Q.-L. Zhang, *Sens. Actuators, B*, 2017, **244**, 77–83.
- B. W. Park, K. A. Ko, D. Y. Yoon and D. S. Kim, *Enzyme Microb. Technol.*, 2012, **51**, 81–85.
- S. Yoo, K. Min, G. Tae and M. S. Han, *Nanoscale*, 2021, **13**, 4467–4474.
- E. M. Gorusuk, B. Bekdeser, M. Bener and R. Apak, *Talanta*, 2020, **218**, 121212.
- Y. Xiong, S. Chen, F. Ye, L. Su, C. Zhang, S. Shen and S. Zhao, *Chem. Commun.*, 2015, **51**, 4635–4638.
- D. Wu, A. C. Sedgwick, T. Gunnlaugsson, E. U. Akkaya, J. Yoon and T. D. James, *Chem. Soc. Rev.*, 2017, **46**, 7105–7123.
- J. Yan, S. Lee, A. Zhang and J. Yoon, *Chem. Soc. Rev.*, 2018, **47**, 6900–6916.
- N. Bouaicha, I. Maatouk, G. Vincent and Y. Levi, *Food Chem. Toxicol.*, 2002, **40**, 1677–1683.
- A. Asati, C. Kaittanis, S. Santra and J. M. Perez, *Anal. Chem.*, 2011, **83**, 2547–2553.
- P. Khan, D. Idrees, M. A. Moxley, J. A. Corbett, F. Ahmad, G. von Figura, W. S. Sly, A. Waheed and M. I. Hassan, *Appl. Biochem. Biotechnol.*, 2014, **173**, 333–355.
- B. Zhao, F. A. Summers and R. P. Mason, *Free Radicals Biol. Med.*, 2012, **53**, 1080–1087.
- C. S. Karamitros, J. Lim and M. Konrad, *Anal. Biochem.*, 2014, **445**, 20–23.
- E. N. Kadnikova and N. M. Kostić, *J. Mol. Catal. B: Enzym.*, 2002, **18**, 39–48.
- R. J. Petroski, *Synth. Commun.*, 2006, **36**, 1727–1734.
- S. Stanković and J. H. Espenson, *Chem. Commun.*, 1998, 1579–1580.
- H. Rudler, B. Denise and S. Masi, *C. R. Acad. Sci., Ser. IIC: Chim.*, 2000, **3**, 793–801.
- P. Anbarasan, H. Neumann and M. Beller, *Chem*, 2011, **17**, 4217–4222.
- L. Gao, J. Zhuang, L. Nie, J. Zhang, Y. Zhang, N. Gu, T. Wang, J. Feng, D. Yang and S. Perrett, *Nat. Nanotechnol.*, 2007, **2**, 577–583.
- V. Balasubramanian, A. Correia, H. Zhang, F. Fontana, E. Makila, J. Salonen, J. Hirvonen and H. A. Santos, *Adv. Mater.*, 2017, **29**, 1605375.
- Y. Z. Li and A. Townshend, *Anal. Chim. Acta*, 1997, **340**, 159–168.
- X.-L. Chena, D.-H. Li, H.-H. Yang, Q.-Z. Zhua, H. Zheng and J.-G. Xua, *Anal. Chim. Acta*, 2001, **434**, 51–58.
- J. Meyer, A. Büldt, M. Vogel and U. Karst, *Angew. Chem., Int. Ed.*, 2000, **39**, 1453–1455.
- H. Akhavan-Tafti, R. deSilva, R. Eickholt, R. Handley, M. Mazelis and M. Sandison, *Talanta*, 2003, **60**, 345–354.

